URSI GASS 2021, Rome, Italy, 28 August - 4 September 2021

Use of sparsity in nonlinear electromagnetic imaging: wavelet-based contrast source method

Yarui Zhang(1), Marc Lambert(1), Aurélia Fraysse(2), and Dominique Lesselier(2)
(1) Université Paris-Saclay, CentraleSupélec, CNRS, Laboratoire de Génie Electrique et Electronique de Paris, 91192, Gif-sur-Yvette, France.
Sorbonne Université, CNRS, Laboratoire de Génie Electrique et Electronique de Paris, 75252, Paris, France
(2) Université Paris-Saclay, CNRS, CentraleSupélec, Laboratoire des signaux et systèmes, 91190, Gif-sur-Yvette, France

Abstract

A contrast source inversion (CSI) algorithm is developed in the wavelet domain in order to tackle nonlinear electromagnetic inverse scattering with the benefit of sparsity. The soft-thresholding technique is applied here to sparsify the reconstruction. Numerical results show the potential of the proposed approach to improve the quality of reconstruction compared to the original CSI method.

1 Introduction

Electromagnetic inverse scattering problems have to be tackled in order to get the geometry and/or the distribution of physical parameters of an object from the knowledge of fields it scatters (see [1, 2]). Various inversion methods have been proposed, such as Born iterative method (BIM) [3], contrast source inversion (CSI) [4] and subspace-based optimization method (SOM) [5]. Due to the use of the nonlinear integral equation and the lack of information, electromagnetic inverse scattering problems usually suffer from non-linearity and ill-posedness. The implementation of stable and effective algorithms is challenging.

The wavelet bases are often used to represent a given profile with low number of non-zero coefficients without a significant loss of resolution, and the incorporation of the wavelet transform into classical inversion methods has been much investigated. In [6], the unknown contrast and induced current are represented using a wavelet basis and updated with multiplicative regularized CSI method, which greatly improves the performance compared to CSI in the spatial domain. The SOM method has also been applied in the wavelet domain in [7]. The performance of different wavelet bases has been analyzed and it has been proved that the use of wavelet transform can improve the resolution of specific region of a scatterer. In [8], a wavelet-based joint ℓ_1–ℓ_2 norm minimization technique within the BIM framework has been proposed.

Our work aims at developing a CSI method in the wavelet domain, at the same time, incorporating the sparsity into this framework due to the great potential of sparsity to effectively tackle the inverse problem and its robustness to noise [10]. To this end, the contrast function and the equivalent current are both represented and updated in the wavelet domain, by minimizing the cost function in the wavelet domain using the conjugate-gradient (CG) method. Herein, the sparsity is enforced on the wavelet coefficients using the soft-thresholding technique.

This contribution is organized as follows. The formulation of the forward problem is considered in Section 2. The original CSI method and its application in the wavelet domain is provided in Section 3. In Section 4, numerical results are discussed including the comparison between original CSI and wavelet-domain CSI. In Section 5, conclusions are given and future research topics discussed.

2 Formulation of the forward problem

Herein, the scenario in Fig. 1 is considered. We focus on a time-harmonic two-dimensional (2D) electromagnetic scattering problem for transverse magnetic (TM) polarization. The object is embedded in a homogeneous medium D with permittivity of air ε_0 and permeability μ_0. Denote $\varepsilon_r(\mathbf{r})$ and $\sigma(\mathbf{r})$ the relative permittivity and conductivity of the medium as $\mathbf{r} \in D$ is an observation point. The object is illuminated by TM waves generated by N_s sources located at positions $\mathbf{r}_s$. For each illumination, the scattered fields are collected by N_r receivers located at positions $\mathbf{r}_r$ on a line of observation S. Time convention is assumed as $e^{-i\omega t}$, ω the angular frequency.

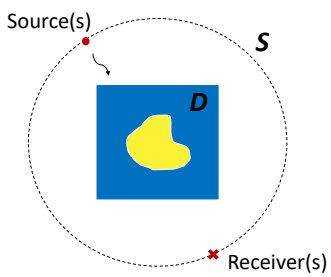

Figure 1. Configuration of the inverse scattering problem and the source-receiver locations

The scattered electric field $E^{\text{diff}}(\mathbf{r}_r, \mathbf{r}_s)$ collected by a receiver placed at $\mathbf{r}_r$ and associated with the source placed at

$\mathbf{r}_s$ satisfies the integral equation

$$E^{\text{diff}}(\mathbf{r}_r,\mathbf{r}_s) = \int_D G(\mathbf{r}_r,\mathbf{r}')J(\mathbf{r}',\mathbf{r_s})d\mathbf{r}' \quad (1)$$

with

$$J(\mathbf{r},\mathbf{r_s}) = \chi(\mathbf{r})E(\mathbf{r},\mathbf{r}_s) \quad (2)$$

$G(\mathbf{r},\mathbf{r}')$ is the Green's function which represents the electromagnetic response to a line source radiating in free-space. In the case of two dimensions, it is given by $G(\mathbf{r},\mathbf{r}') = \frac{-i\omega\mu_0}{4}\mathrm{H}_0^{(1)}(k_B\|\mathbf{r}-\mathbf{r}'\|)$, where $\mathrm{H}_0^{(1)}$ is the zero-order Hankel function of the first kind.

The contrast function $\chi(\mathbf{r})$ is defined as $k^2(\mathbf{r}) - k_B^2$, where $k^2(\mathbf{r}) = \omega^2\varepsilon_0\varepsilon_r(\mathbf{r})\mu_0 + i\omega\mu_0\sigma(\mathbf{r})$, $k_B^2 = \omega^2\varepsilon_0\mu_0$. $J(\mathbf{r},\mathbf{r_s})$ and $E(\mathbf{r},\mathbf{r}_s)$ are the equivalent current and the total electric field respectively, both induced within the object by the incident wave.

The total electric field can be obtained according to

$$E(\mathbf{r},\mathbf{r_s}) = E^{\text{inc}}(\mathbf{r},\mathbf{r}_s) + \int_D G(\mathbf{r},\mathbf{r}')J(\mathbf{r}',\mathbf{r_s})d\mathbf{r}' \ \forall\mathbf{r}\in D \quad (3)$$

where $E^{\text{inc}}(\mathbf{r},\mathbf{r}_s)$ is the incident field. Using a method of moments, the domain D is discretized in N small square pixels so that the electric field and the contrast can be considered as constants within each one. The discretized version of the previous equations stands as

$$E_i^{\text{diff}}(\mathbf{r}) = G_S J_i(\mathbf{r}) \qquad i = 1,\dots,N_s \qquad \mathbf{r}\in S \quad (4)$$

$$E_i(\mathbf{r}) = E_i^{\text{inc}}(\mathbf{r}) + G_D J_i(\mathbf{r}) \qquad i = 1,\dots,N_s \qquad \mathbf{r}\in D \quad (5)$$

where $E_i^{\text{diff}}(\mathbf{r})$ is a complex vector of size N_r, and $E_i^{\text{inc}}(\mathbf{r})$, $E_i(\mathbf{r})$ are complex vectors of size N. G_S is a complex matrix of size $N_r\times N$, G_D a matrix of size $N\times N$. The subscripts D and S of the operators indicate the location of the point $\mathbf{r}$, and the operators are identical in all other aspects:

$$G_{D,\,S}J_i(\mathbf{r}) = k_B^2\int_D G(\mathbf{r},\mathbf{r}')J_i(\mathbf{r}')d\mathbf{r}' \qquad \mathbf{r}\in D \text{ or } \mathbf{r}\in S \quad (6)$$

The forward problem is defined as the calculation of $E_i^{\text{diff}}(\mathbf{r})$ from the knowledge of $\chi(\mathbf{r})$ and the inverse scattering problem is to retrieve $\chi(\mathbf{r})$ from $E_i^{\text{diff}}(\mathbf{r})$, which is nonlinear and ill-posed.

3 Wavelet-domain contrast source inversion method

The CSI method is one of the most used methods to tackle the inverse scattering problem. First, by combining Eq. (2) and (5), the state equation is defined as

$$J_i(\mathbf{r}) = \chi(\mathbf{r})[E_i^{\text{inc}}(\mathbf{r}) + G_D(J_i(\mathbf{r}))] \qquad \mathbf{r}\in D \quad (7)$$

and the data equation as

$$f_i(\mathbf{r}) = G_S J_i(\mathbf{r}) \qquad \mathbf{r}\in S \quad (8)$$

The cost function is a combination of two normalized terms:

$$F(J_1,\dots J_{N_s},\chi) = \frac{\sum_{i=1}^{N_s}\|f_i - G_S(J_i)\|_S^2}{\sum_{i=1}^{N_s}\|f_i\|_S^2} + \frac{\sum_{i=1}^{N_s}\|\chi E_i^{\text{inc}} + \chi G_D(J_i) - J_i\|_D^2}{\sum_{i=1}^{N_s}\|\chi E_i^{\text{inc}}\|_D^2} \quad (9)$$

where $\|\cdot\|_S^2$ and $\|\cdot\|_D^2$ denote the norms on $L^2(S)$ and $L^2(D)$, respectively.

The CSI method alternatively constructs sequences of contrast sources $J_{i,k}$ ($i = 1,\dots,N_s, k = 1,\dots,K$ where K is the number of iterations) by a conjugate gradient iterative method such that the contrast sources minimize the cost functional, and the contrast χ_i is then determined by minimizing the error in the state equation. The initial guess for the contrast source and of the contrast function is obtained by back-propagation:

$$J_{i,1}^{\text{bp}} = \frac{\|G_S^* f_i\|_D^2}{\|G_S G_S^* f_i\|_S^2} G_S^* f_i \quad (10)$$

$$\chi_k = \frac{\sum_i J_{i,1}\overline{E}_{i,1}}{\sum_i |E_{i,1}|^2} \quad (11)$$

Inspired from [6], we can apply the CSI method in the wavelet domain. First, let us define the wavelet transform as $\mathcal{W}$ and its inverse as $\mathcal{W}^*$. $\|\cdot\|_{Dw}^2$ and $\|\cdot\|_{Sw}^2$ indicate the norms on $L^2(S)$ and $L^2(D)$ in the wavelet domain. The data equation and the state equation can be written as

$$f_i = G_S(\mathcal{W}^*\gamma_i) \quad (12)$$

$$\gamma_i = \mathcal{W}\{(\mathcal{W}^*\beta)E_i^{\text{inc}}\} + \mathcal{W}\{(\mathcal{W}^*\beta)G_D(\mathcal{W}^*\gamma_i)\} \quad (13)$$

where $\gamma_i = \mathcal{W}J_i$, $\beta = \mathcal{W}\chi$.

Now, let us define the data error as

$$\rho_i = f_i - G_S(\mathcal{W}^*\gamma) \quad (14)$$

and the object error as

$$r_i = \mathcal{W}\{(\mathcal{W}^*\beta)E_i^{\text{inc}}\} - \gamma_i + \mathcal{W}\{(\mathcal{W}^*\beta)G_D(\mathcal{W}^*\gamma_i)\} \quad (15)$$

The CSI cost function in the wavelet domain is given by

$$F(\gamma_1,\dots\gamma_{N_s},\beta) = \frac{\sum_{i=1}^{N_s}\|f_i - G_S(\mathcal{W}^*\gamma_i)\|_{Sw}^2}{\sum_{i=1}^{N_s}\|f_i\|_{Sw}^2} + \frac{\sum_{i=1}^{N_s}\|\mathcal{W}\{(\mathcal{W}^*\beta)E_i^{\text{inc}}\} + \mathcal{W}\{(\mathcal{W}^*\beta)G_D(\mathcal{W}^*\gamma_i)\} - \gamma_i\|_{Dw}^2}{\sum_{i=1}^{N_s}\|\mathcal{W}\{(\mathcal{W}^*\beta)E_i^{\text{inc}}\}\|_{Dw}^2} \quad (16)$$

Then, $\gamma_{i,k}$ and β_i are constructed alternatively by minimizing the wavelet-domain cost function. A summary of the CSI method in the wavelet domain is in the algorithm below.

By applying the wavelet transform on the contrast source and the contrast function, two sets of decomposition coefficients can be obtained: approximation and detail coefficients. The approximation coefficients describe the general form of the profile, while detail coefficients represent the finer details of the profile. Our goal is to enforce the sparsity on the detail coefficients.

Algorithm Contrast source inversion in the wavelet domain

Initialize $\gamma_{i,1}^{bp} = \mathcal{W}\left\{\frac{\|G_S^* f_i\|_D^2}{\|G_S G_S^* f_i\|_S^2} G_S^* f_i\right\}$

$\beta_{i,0} = \mathcal{W}\left\{\frac{\sum_i (\mathcal{W}^* \gamma_{i,0}) \overline{E}_{i,0}}{\sum_i |E_{i,0}|^2}\right\}$

Compute the normalization coefficients

$\eta_S = (\sum_i \|f_i\|_{Sw}^2)^{-1}$

for $k = 1, \ldots, K$ **do**

  Compute the normalization coefficients

  $\eta_{D,k} = \sum_i \|\mathcal{W}\{(\mathcal{W}^* \beta_k) E_i^{\text{inc}}\}\|_{Dw}^2$

  Updating of the Contrast Sources

  Compute the gradient

  $g_{i,k}^J = -\eta_S \mathcal{W}\{G_S^* \rho_{i,k}\} - \eta_{D,k}\{r_{i,k} - \mathcal{W} G_D^*(\overline{\mathcal{W}^* \beta_k})(\mathcal{W}^* r_{i,k})]\}$

  Compute the update direction $v_{i,k} = g_{i,k}^J + \frac{Re \sum_i < g_{i,k}^J, g_{i,k}^J - g_{i,k-1}^J >_{Dw}}{\sum_i < g_{i,k-1}^J, g_{i,k-1}^J >_{Dw}} v_{i,k-1}$

  Determine the step size $\alpha_k^J = \frac{-Re \sum_i < g_{i,k}^J, v_{i,k} >_{Dw}}{\eta_S \sum_i \|G_S(\mathcal{W}^* v_{i,k})\|_S^2 + \eta_{D,k} \sum_i \|v_{i,k} - \mathcal{W}\{(\mathcal{W}^* \beta_k) G_D(\mathcal{W}^* v_{i,k})\}\|_{Dw}^2}$

  Update $\gamma_{i,k}$ by $\gamma_{i,k} = \gamma_{i,k-1} + \alpha_k^J v_{i,k}$

  Updating of the Contrast

  Update the field $E_{i,k} = E_{i,k}^{\text{inc}} + G_D(\mathcal{W}^* \gamma_{i,k})$

  Update β_k by $\beta_k = \mathcal{W}\left\{\frac{\sum_i (\mathcal{W}^* \gamma_{i,k}) \overline{E}_{i,k}}{\sum_i |E_{i,k}|^2}\right\}$

  Check stopping criterion

end for

Consider an approximation coefficient as a *parent* coefficient, all detail coefficients of the same orientation in the same spatial location are defined as its *children* coefficients. According to [9], a wavelet coefficient x is said to be insignificant with respect to a given threshold T_1 if $|x| < T_1$. If a *parent* coefficient is insignificant, then all of its *children* coefficients are said to be insignificant. Through this relationship, the positions of significant detail coefficients of an image can be determined from its approximation coefficients.

The first step of our approach is to update only approximation coefficients to obtain a preliminary result. Then, the positions of significant wavelet coefficients can be determined based on this result. The second step is to launch again the algorithm to update the significant detail coefficients and to get a finer result with the previous result being the initial model. At the same time, the soft-thresholding is applied to set to zero the elements whose absolute values are lower than the threshold value T_2 and then to shrink the non-zero detail coefficients toward zero.

4 Numerical results

In the numerical simulations, the well-known "Austria" profile which contains two disks and one ring is used. The disks of radius 0.2 m are centered at $(0.3, 0.6)$ m and $(-0.3, 0.6)$ m. The ring has an exterior radius of 0.6 m and an inner radius of 0.3 m, and is centered at $(0, 0.2)$ m. The true value of the relative permittivity of the object is 2, and it is 1 for the embedding medium.

The region of interest D is $l = 1.33\lambda$ sided where λ is the wavelength in air, and it is discretized into $N_x \times N_y = N$ square cells. The discretization sizes for the direct and inverse problem are different in order to avoid the "inverse crime". Each cell is collected from N_r receivers when illuminated by N_s transmitters at 500 MHz frequency. The transmitters and receivers are evenly distributed on a circle of radius $r = 2.5\lambda$. Gaussian noise with SNR of 20 dB is added to the data. In our simulations, we have also applied positivity constraint by projection method [4]. The wavelet basis used in the simulations is the Haar wavelet, and the level of wavelet decomposition $J = 1$. The threshold value T_1 is the $85th$ percentile of approximation coefficients, and T_2 is set to the minimum value of the significant approximation coefficients.

In the following, three methods are discussed including spatial-domain CSI, wavelet-domain CSI using all coefficients and wavelet-domain CSI using only significant wavelet coefficients with the soft-thresholding step respectively named as CSI, W-CSI and W-CSI-ST. In order to evaluate the performance of the reconstruction, we define the relative error as

$$err = \frac{\|\chi_{\text{reconstructed}} - \chi_{\text{true}}\|^2}{\|\chi_{\text{true}}\|^2} \tag{17}$$

Table 1 shows the relative error err of the discussed methods. We can see from the result that the proposed method ensures better quality of reconstruction when N_s and N_r are small but about the same quality (at the price of increasing CPU time) when N_s and N_r increase. In addition, a statistical study was carried out on 100 samples of err obtained

Table 1. Errors of reconstruction err with different $\{N_s \times N_r\}$

$N_s \times N_r$	CSI	W-CSI	W-CSI-ST
6×18	0.3390	0.4150	**0.2038**
9×18	0.1798	0.1852	**0.1738**
12×18	**0.0981**	0.1200	0.1263
8×32	**0.1192**	0.1239	0.1379
16×32	**0.0869**	0.1012	0.1172

using three methods with small N_s and N_r, and WT-CSI-ST gave the lowest *err* in every single test.

As an illustration, a comparison of the final results for $N_s = 6$ and $N_r = 18$ is shown in Fig. 2. As expected, W-CSI-ST (Fig. 2d) provides a better and smoother results than CSI (Fig. 2b) and W-CSI (Fig. 2c) when using a small number of sources and receivers at a CPU time cost of 150 s for $K = 500$ compared to 22 s and 75 s respectively. The machine that has been used has a processor such as: Intel Core i9 CPU@2.9 GHz.

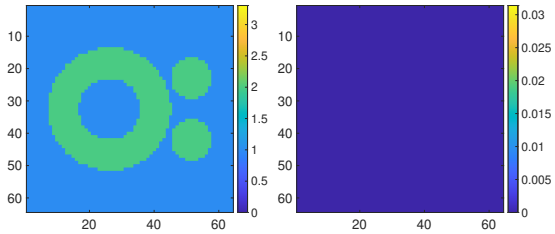

(a) Ground truth

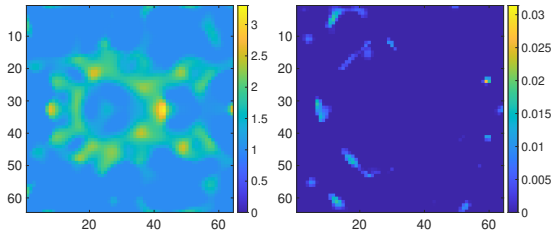

(b) CSI

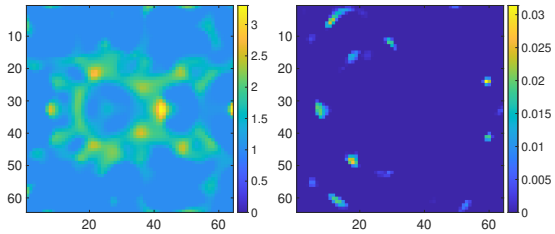

(c) W-CSI

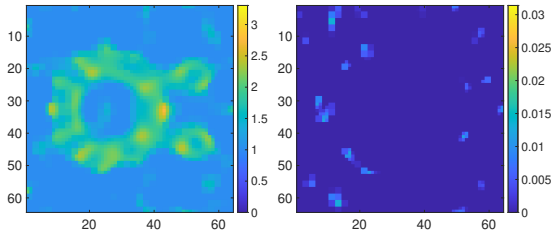

(d) W-CSI-ST

Figure 2. Real (left) and imaginary (right) parts of true model (a), and reconstructed model using CSI (b) and wavelet-domain CSI without (c) and with sparsity constraint (d) for $N_s = 6$ and $N_r = 18$.

5 Conclusion and future work

A new approach has been proposed in order to solve the inverse scattering problem with strong non-linearity by enforcing the sparsity through the soft thresholding in the wavelet domain. The proposed approach has been compared with the original CSI method and the wavelet-domain CSI method without soft-thresholding step. As the situation is strongly nonlinear, both algorithms are not able to reconstruct the profile perfectly. However, the use of sparsity in the wavelet domain does improve the quality of reconstruction. Future research will be on the accurate determination of hyperparameters and the test of other wavelet bases such as the Daubechies 4.

References

[1] X. Chen, *Computational Methods for Electromagnetic Inverse Scattering,* John Wiley & Sons, Ltd, 2018.

[2] M. Pastorino and A. Randazzo, *Microwave Imaging Methods and Applications*, Artech House, 2018.

[3] Y. M. Wang and W. C. Chew, "An Iterative Solution of the Two-dimensional Electromagnetic Inverse Scattering Problem," *International Journal of Imaging Systems and Technology* **1**, pp. 100–108, 1989, doi: 10.1002/ima.1850010111.

[4] P. M. van den Berg and A. Abubakar, "Contrast Source Inversion Method: State of Art," *Progress In Electromagnetics Research*, **34**, pp. 189-218, 2001. doi: 10.2528/PIER01061103.

[5] X. Chen, "Subspace-Based Optimization Method for Solving Inverse-Scattering Problems," *IEEE Transactions on Geoscience and Remote Sensing*, **48**, 1, pp. 42-49, 2010, doi: 10.1109/TGRS.2009.2025122.

[6] M. Li, O. Semerci, and A. Abubakar, "A Contrast Source Inversion Method in the Wavelet Domain," *Inverse Problems*. **29**, 025015, 2013, doi: 10.1088/0266-5611/29/2/025015.

[7] T. Yin, Z. Wei, and X. Chen, "Wavelet Transform Subspace-Based Optimization Method for Inverse Scattering," *IEEE Journal on Multiscale and Multiphysics Computational Techniques*, **3**, pp. 176-184, 2018, doi: 10.1109/JMMCT.2018.2878483.

[8] Y. Sanghvi, H. Bisht, U. Khankhoje, V. Gadre, and S. Kulkarni, "Iteratively Reweighted $\ell 1 - \ell 2$ Norm Minimization using Wavelets in Inverse Scattering," *Journal of the Optical Society of America A*, **37**, pp. 889-889, 2020, doi: 10.1364/JOSAA.396227.

[9] J. M. Shapiro, "Embedded Image Coding using Zerotrees of Wavelet Coefficients," *IEEE Transactions on Signal Processing*, **41**, 12, pp. 3445-3462, 1993, doi: 10.1109/78.258085.

[10] H. Zaimaga, A. Fraysse, and M. Lambert, "Sparse Reconstruction Algorithms for Nonlinear Microwave Imaging," *25th European Signal Processing Conference (EUSIPCO)*, Kos, 2017, pp. 713-717, doi: 10.23919/EUSIPCO.2017.8081300.